Life Sciences 361 (2025) 123298

Contents lists available at ScienceDirect

Life Sciences

journal homepage: www.elsevier.com/locate/lifescie

iPSC-derived mesenchymal stromal cells stimulate neovascularization less than their primary counterparts

Julian Gonzalez-Rubio [a], Kira Zeevaert [b], Eva Miriam Buhl [c], Michaela Schedel [d,e], Stefan Jockenhoevel [a], Christian G. Cornelissen [a,f], Wolfgang Wagner [b], Anja Lena Thiebes [a,*]

[a] Department of Biohybrid & Medical Textiles (BioTex), AME - Institute of Applied Medical Engineering, Helmholtz Institute, RWTH Aachen University, 52074 Aachen, Germany
[b] Institute of Stem Cell Biology, Helmholtz Institute for Biomedical Engineering, RWTH Aachen University Medical School, 52074 Aachen, Germany
[c] Institute of Pathology, Electron Microscopy Facility, RWTH Aachen University Hospital, 52074 Aachen, Germany
[d] Department of Pulmonary Medicine, University Medicine Essen-Ruhrlandklinik, 45239 Essen, Germany
[e] Department of Pulmonary Medicine, University Medicine Essen, 45147 Essen, Germany
[f] Clinic for Pneumology and Internal Intensive Care Medicine (Medical Clinic V), RWTH Aachen University Hospital, 52074 Aachen, Germany

ARTICLE INFO

Keywords:
Angiogenesis
Vasculogenesis
Induced pluripotent stem cells
Cell therapy
Organ-on-a-chip
In vitro model

ABSTRACT

Aims: Mesenchymal stromal cells (MSCs) are being tested and accepted as a source for cell therapy worldwide. However, the advanced age of the patients, together with the difficulties in achieving the required cell amounts, impede autologous treatments. Reprogramming of MSCs into induced pluripotent stem cells (iPSCs), followed by re-differentiation to MSCs has emerged as a promising and safe method to facilitate the cell expansion and the removal of aging-associated characteristics. However, the effect of reprogramming on the MSC's pro-angiogenicity is poorly understood.
Materials and methods: In this study, we use a microfluidic organ-on-a-chip platform designed for vascularization assays to study and compare the effects of bone marrow MSCs (BM-MSCs) and iPSC-derived MSCs (iMSCs) in stimulating the formation of vessels by endothelial cells. Cells were loaded in fibrin hydrogels, injected into the microfluidic channel, and grown for ten days.
Key findings: Fluorescence microscopy revealed that BM-MSCs promote the formation of long and interconnected endothelial vessels, while iMSCs barely stimulate neoangiogenesis. This was further confirmed and explained by bulk RNA sequencing, showing a decrease of pro-angiogenic agents in both of the iMSCs co-cultures. Furthermore, transmission electron microscopy revealed that BM-MSCs closely associate with the new vessels as perivascular cells, while iMSCs just remain in proximity.
Significance: These results highlight iMSCs as a promising substitute for BM-MSCs in the treatment of diseases with pernicious vascularization, such as osteoarthritis, ocular degeneration, and cancer.

1. Introduction

Mesenchymal stromal cells (MSCs) are a heterogeneous mixture of plastic-adherent cells that can be isolated from connective tissue of different origins, such as bone marrow, adipose tissue, or umbilical cord [1]. Firstly isolated from the bone marrow by Alexander Friedenstein and colleagues in the 1960s, these cells caught the attention of the scientific community due to their capacity to be differentiated *in vitro* into other mesoderm-derived cells such as adipocytes, osteoblasts, or chondrocytes [2,3]. However, most of the clinical applications employing MSCs are not based on this trans-differentiation potential but rely on their immunomodulatory and pro-regenerative properties [4]. Over the past decade, more than a thousand clinical trials have been initiated for diseases as diverse as graft-*versus*-host rejection, diabetes, and multiple sclerosis [5]. Most of these diseases have a high comorbidity with aging, and therefore autologous MSCs from these patients usually present a low division rate and senescence markers, which can decrease their therapeutic potential and impede the already complex task of reaching the number of cells needed to treat an adult [6].

Reprogramming of primary MSCs into induced pluripotent stem cells (iPSCs) followed by a re-differentiation towards MSCs (iMSCs) erases age-related epigenetic markers related to senescence [7–9]. This

* Corresponding author.
E-mail address: thiebes@ame.rwth-aachen.de (A.L. Thiebes).

https://doi.org/10.1016/j.lfs.2024.123298
Received 15 October 2024; Received in revised form 29 November 2024; Accepted 2 December 2024
Available online 6 December 2024

"rejuvenation" might improve treatment outcomes without compromising their safety [6]. Furthermore, since iPSCs can be cultured and expanded without any signs of senescence, this procedure may give rise to unlimited numbers of iMSCs, and a possibly more homogeneous composition.

However, it is still unclear if the newly derived MSCs possess the same characteristics as the original ones [7]. Due to their tissue origin, MSCs from tissues such as the bone marrow have a tight relation with blood capillaries, showing a strong ability to induce neovascularization [10]. Nevertheless, the growth of new vessels is associated with poor prognosis in diseases such as osteoarthritis, wet age-related macular degeneration, cancer, and others, which are also some of the most studied conditions in MSC therapy trials [11]. So far, the impact of reprogramming and re-differentiation on the pro-angiogenic potential of the MSCs has not been systematically addressed.

In this study, we aim to explore the effect of iPSC-derived MSCs on neovascularization compared to non-reprogrammed primary MSCs and reflect on the potential implications for cell therapy trials. For this, we use state-of-the-art microfluidic chips specifically designed for vascularization assays, providing a more physiological environment and optimized visualization.

2. Materials and methods

2.1. Cell isolation and culture

Bone marrow-derived mesenchymal stromal cells (BM-MSCs) were isolated from femoral heads kindly provided by the Clinic for Orthopedic, Trauma and Reconstructive Surgery of the RWTH Aachen University Hospital after informed consent of the patient (ethics approval: EK 300/13). The inner part of the bone was punctured several times with a bone marrow biopsy needle filled with Mesenpan media (Pan-Biotech, Aidenbach, Germany) supplemented with 2 % fetal bovine serum (FBS; Gibco, Dreieich, Germany) and 1 % antibiotic/antimycotic solution (ABM; mixture of 10,000 U/mL penicillin, 10,000 μg/mL streptomycin and 25 μg/mL Amphotericin B; Gibco, Dreieich, Germany) over a sterile petri dish. Part of the media was extruded after every perforation to wash off the cells released by the crushing, which were then collected with another syringe. The cell suspension was added in a falcon tube and centrifuged for 5 min at 500*g*. The supernatant was removed. The pellet was resuspended in Mesenpan media supplemented with 2 % FBS and 1 % ABM and added to a T75 cell culture flask.

To isolate human umbilical vein endothelial cells (HUVECs), umbilical cords provided by the centralized Biomaterial Bank of RWTH Aachen University after informed consent of the mother (cBMB project number 323; supported by the Clinic for Gynecology and Obstetrics, RWTH Aachen University Hospital) were clamped in one end and filled with 400 U/mL collagenase type I (Sigma-Aldrich, Darmstadt, Germany) through the vein using a blunt cannula. The umbilical cord was then incubated for 30 min at 37 °C to digest and release the endothelial cells lining the vessel. The vein was then unclamped and flushed with PBS to remove the dissociated endothelial cells, which were collected and centrifuged at 500*g* for 5 min. T75 cell-culture flasks were coated with a solution of 2 % gelatine from bovine skin (Sigma-Aldrich, Darmstadt, Germany) and incubated for 30 min at room temperature (RT). The pellet was resuspended in EGM2 media (PromoCell Heidelberg, Germany) supplemented with 1 % ABM, and transferred to the gelatine-coated flasks.

All cells were cultured in a humidified incubator at 37 °C with 5 % CO2 and 20 % O2. Media was exchanged every 48–72 h. Cells were trypsinized and passaged in a 1:4 dilution when reaching a 70–90 % confluency. Both BM-MSCs and HUVECs were frozen in liquid nitrogen in a freezing solution composed of 80 % (*v*/v) Dulbecco's Modified Eagle Medium (DMEM; Gibco, Dreieich, Germany), 10 % (v/v) FBS, and 10 % (v/v) dimethyl sulfoxide (DMSO; Sigma-Aldrich, Darmstadt, Germany) until further use.

2.2. iPSC reprogramming and culture

Three human iPSC lines were generated from BM-MSCs (hPSCreg: UKAi009-A (iPSC 102), UKAi010-A (iPSC 104), and UKAi011-A (iPSC 106)) by reprogramming with episomal plasmids as previously described [12]. All samples were taken after informed consent of the patient using guidelines approved by the Ethics Committee for the Use of Human Subjects at the RWTH Aachen University (EK 128/09). Pluripotency of iPSCs was validated by three lineage differentiation potentials and Epi-Pluri-Score analysis, as previously described [12,13].

The iPSC lines were cultured under sterile conditions on tissue culture plastic coated with 0.5 μg/cm^2 vitronectin (Stemcell Technologies, Vancouver, Canada) in StemMACS iPS-Brew XF (Miltenyi Biotec GmbH, Bergisch Gladbach, Germany) supplemented with 100 U/mL penicillin/streptomycin (Gibco, Dreieich, Germany) Medium change was performed daily. Cells were passaged at a confluency of 70–90 %. For passaging, media was aspirated from the well and cells were incubated with 1 mL ethylenediaminetetraacetic acid (EDTA; 0.5 mM; Life Technologies, Dreieich, Germany) for 3–4 min at RT. EDTA was removed and colonies were gently detached with StemMACS iPS-Brew XF (Miltenyi, Bergisch Gladbach, Germany) and transferred to a new vitronectin-coated well plate. Depending on the clone-specific proliferation rate, cells were passaged in a ratio of 1:6 to 1:12.

2.3. iPSC-derived MSCs generation

For differentiation of iPSCs towards iMSCs, singularized iPSCs were seeded with 10,000 cells/cm^2 in StemMACS iPS-Brew XF with Rho-kinase (ROCK) inhibitor (Y-27632; 10 μM; Abcam, Cambridge, UK) on vitronectin-coated plates. At 50 to 60 % confluency, media was changed to human platelet lysate (hPL) media, containing DMEM Low Glucose (Sigma-Aldrich, Darmstadt, Germany), 10 % *v*/v hPL-pool [14], 0.1 % v/v heparin (5 U/mL), 2 mM L-glutamine, and 100 U/mL penicillin/streptomycin solution causing mesodermal differentiation from the initial colonies. Cells were further cultured for 35 days and media was changed every 2 to 3 days. iMSC passaging was performed once a week by singularizing with 1 mL trypsin-EDTA 0.25 % (Gibco, Dreieich, Germany) for 5 min at 37 °C and seeding with 40,000 cells/cm^2. For passages one and two, cells were cultured on 0.1 % *w/v* gelatin-coated plates. From passage three, cells were plastic-adherent and cultured without substrate coating. iMSCs were frozen in hPL-medium with 10 % DMSO.

2.4. Flow cytometry

The immunophenotypic analysis by flow cytometry of iMSCs in comparison to primary BM-MSCs and iPSCs was performed for the surface markers CD29, CD73, CD90, CD105, CD14, CD31, CD34, and CD45 with a FACSCanto II cytometer (BD Biosciences, Franklin Lakes, USA).

Cells were detached with Accutase (for iPSCs; Stemcell Technologies, Vancouver, Canada) or Trypsin-EDTA (for BM-MSCs/iMSCs) as previously described and 1 × 10^6 cells were resuspended in 5 mL of FACS buffer (PBS with 2 % FBS), followed by the addition of antibodies to 1 mL of the containing solution at a 1:333 dilution (complete list of antibodies in Supplementary Table 1). This mixture was incubated for 30 mins at 4 °C. After incubation, cells were centrifuged again, the supernatant was carefully discarded, and the cells were resuspended in 0.5 mL of FACS buffer for each experimental condition. The samples were kept on ice until flow cytometry analysis. A control sample without antibodies was prepared to assess cellular autofluorescence. The data was processed and analyzed using FlowJo (Becton Dickinson, Franklin Lakes, USA).

2.5. Preparation of the gels

Lyophilized fibrinogen from human plasma (VWR, Darmstadt,

Germany) was dissolved in ultrapure water and dialyzed against Tris-buffered saline (TBS; prepared in-house) overnight within a Spectra/Por 1 tubing (Fisher Scientific, Schwerte, Germany) with a molecular weight cut-off of 6–8 kDa. Fibrinogen was sterilized by filtration and the concentration was determined by measuring absorbance at 280 nm using a M200 spectrophotometer (Tecan, Männedorf, Switzerland). The fibrinogen was kept frozen at −80 °C until further use. Before the chip preparation, the fibrinogen was thawed and diluted to 10 mg/mL in TBS. Thrombin from bovine plasma and calcium chloride (both Sigma-Aldrich, Darmstadt, Germany) were solved in TBS to prepare the polymerizing solution. BM-MSCs, iMSCs, and HUVECs were washed with sterile PBS, treated with trypsin (Pan-Biotech, Aidenbach, Germany) for 5 min, detached from the cell culture flask, and counted using a Neubauer chamber (Brand, Wertheim, Germany). Then, cells were suspended in the polymerizing solution, reaching a final concentration of 6 IU/mL thrombin, 7.5 mM calcium chloride, 20×10^6 HUVECs, and 4×10^6 BM-MSCs/iMSCs. 5 μL of the fibrinogen was mixed with 5 μL of the cell suspension and quickly injected in the inner chip's channel (idenTx 3 Chip, AIM Biotech, Singapore), halving the concentration of each component. The chips were incubated for 20 min at RT and for another 20 min in a humidified incubator at 37 °C and 5 % CO_2 to allow for full polymerization. Finally, the lateral channels were filled with EGM MV2 media (PromoCell, Heidelberg, Germany) supplemented with 1 % ABM, adding 100 μL to the bottom left well, 80 μL to the bottom right well, 60 μL to the top left well and 40 μL to the top right well. Adding uneven amounts of media in the parallel channels generates a gravity-driven interstitial flow through the gel which improves media replenishment [15]. The media was changed every day for the next ten days until fixation. To prepare the gels for transmission electron microscope (TEM) and RNA isolation, 350 μL of the fibrinogen/polymerizing solution mixture was added to a 24-well plate. After polymerization, 500 μL of EGM2 MV was added to the gels and exchanged every 48 h for the next ten days. BM-MSCs/iMSCs and HUVECs in the gels were in passage 6–7 and 4, respectively. Passage numbers of iMSCs are counted from the start of iPSC differentiation.

2.6. Immunofluorescence visualization and analysis

The gels in the chips were fixed by incubation in ice-cold methanol at −20 °C for 10 min. They were washed three times with PBS and stored at 4 °C until staining. Gels were then treated with anti-PECAM-1 mouse antibody (Sigma-Aldrich, Darmstadt, Germany) diluted 1:100 in a solution of 3 % Bovine Serum Albumin (BSA) and 1 % ABM for 48 h at 37 °C. After the incubation, the samples were washed twice for 5 min each and a third time for 8 h to ensure the extraction of all antibodies within the gel. Then, a second solution of 1:400 Alexa Fluor 594 goat anti-mouse (Invitrogen, Darmstadt, Germany) and 1:1000 Phalloidin-iFluor 488 conjugate (Cayman Chemical, Ann Arbor, Michigan) in 3 % BSA and 1 % ABM was added and incubated for an additional 48 h. After three consecutive washings of 5, 10, and 30 min, the gel was stained with a 0.4 μg/mL DAPI solution for 2 h at 37 °C, washed again, and stored at 4 °C.

Chips were imaged using a confocal microscope LSM 980 with Airyscan 2 (Zeiss, Oberkochen, Germany), with a 20× objective. 8 tiles of stacks of 33 slides (total thickness of 100 μm) were generated for each chip and stitched together for further analysis. Imaris 11 (Oxford Instruments, Abingdon, England) was used to render 3D objects from the red channel stacks (PECAM-1, endothelial cell marker), of which the volume was measured. Then, the 3D vessels were mapped with the Filament analyzer to calculate the number of branching points.

2.7. Transmission electron microscopy

Fibrin gels were fixed and stored in a 3 % glutaraldehyde solution at 4 °C for a week. They were then rinsed with 0.1 M Soerensen's phosphate buffer (Merck, Darmstadt, Germany) and fixed with 1 % osmium tetraoxide (Carl Roth, Karlsruhe, Germany) in a 25 mM sucrose buffer (Merck, Darmstadt, Germany). The samples were dehydrated with a series of ethanol dilutions of increasing concentration and immersed in propylene oxide. Each sample was submerged in a 1:1 propylene oxide and Epon resin (Serva, Heidelberg, Germany) mixture for 1 h, incubated for 1 h in pure Epon resin, and embedded in pure Epon at 90 °C for 2 h.

An ultramicrotome (Reichert Ultracut S, Leica, Wetzlar, Germany) equipped with a Diatome diamond knife was used to cut ultrathin sections, ranging from 90 to 100 nm, which were mounted onto Cu/Rh grids (HR23 Maxtaform, Plano). The sections were stained with 0.5 % uranyl acetate and 1 % lead citrate solution (both from EMS, Hatfield, USA) to increase the contrast and imaged using a Zeiss Leo 906 (Carl Zeiss, Oberkochen, Germany) TEM, with an acceleration voltage of 60 kV.

2.8. RNA sequencing

The RNA of endothelial cells and BM-MSCs/iMSCs localized within the fibrin gel was isolated after 10 days in culture. First, 1 mL TRIzol (Invitrogen, Waltham, USA) was added to the samples and incubated for 5 min. The gels were pipetted up and down vigorously until completely dissociated in the TRIzol solution and were then frozen at −20 °C. On the day of isolation, the samples were thawed, mixed with 0.2 mL of chloroform, and thoroughly shaken. This mixture was separated into two phases by centrifugation for 15 min at 12,000 g at 4 °C. The aqueous phase was removed and added to 0.5 mL isopropanol to precipitate the RNA. The mixture was incubated for 10 min at 4 °C, followed by centrifugation at 12,000 *g* for 10 min at 4 °C. A white, gel-like RNA pellet was formed at the bottom of the tube and the supernatant was carefully removed using a pipette. To further purify the RNA, the pellet was resuspended in 1 mL of 75 % ethanol. The sample was briefly vortexed and then centrifuged at 7500 *g* for 5 min at 4 °C. The supernatant was discarded and the RNA pellet was air-dried for 10–15 min until no liquid was left which was then resuspended in RNase-free water.

The 3'mRNA-Seq libraries were generated using the QuantSeq 3'mRNA-Seq v2 Library Prep Kit FWD with UDIs (Lexogen, Vienna, Austria), following the protocol provided by the manufacturer. Before starting library preparation, RNA concentration was determined using the Promega Quantus Fluorometer, and the RNA size distribution was evaluated with an Agilent TapeStation using RNA ScreenTape. After library preparation, RNA quantification and quality checks were performed again, employing the Quantus fluorometer and the Agilent TapeStation (Santa Clara, California) with High Sensitivity D1000 ScreenTape. The libraries were then denatured, diluted, and loaded onto a NextSeq High Output v2.5 flow cell (Illumina, Munich, Germany) over 75 cycles. To enhance base calling accuracy, a 1 % PhiX control library was included. Single-end sequencing was carried out over 75 cycles on the Illumina NextSeq platform, in line with the manufacturer's guidelines. Raw data have been deposited at NCBIs Gene Expression Omnibus (GEO, http://www.ncbi.nlm.nih.gov/geo/, accession number: GSE283749).

2.9. Gene expression analysis

FASTQ files were generated using the bcl2fastq software (Illumina) and processed using Nextflow 23.10.0 [16] with the nf-core/RNA-seq pipeline (Version 3.12) [17]. Lane-level reads were trimmed with Trim Galore 0.6.7 [18] and aligned to the human genome (GRCh39) with STAR 2.7.9a [19]. Gene-level and transcript-level quantification was performed by Salmon v1.10.1 (Patro et al. 2017) and all the posterior analysis was done using custom scripts in R version 4.3.2 with the DESeq2 v.1.32.0 framework [20]. Gene Set Enrichment Analysis (GSEA) was performed using clusterProfiler version 4.6.2, employing hallmark gene sets from MSigDB [21]. Pre-ranked gene lists, generated from differential gene expression analysis, were added to clusterProfiler [22] to identify enriched biological pathways. Results were corrected for

multiple testing, and FDR q-values below 0.05 were considered significant.

2.10. Statistical analysis

All statistic analyses, except the ones related to RNA sequencing, were performed using SPSS Statistics 27 (IBM, Armonk, USA) and plotted in Excel 2016 (Microsoft, Redmond, USA). Both the vessel length/branching points and the soluble protein quantification data were tested for normality with the Shapiro-Wilk test and then compared using an unpaired *t*-test. In all cases, results with *p*-values below 0.05 were considered significant.

3. Results

3.1. iPSC-MSCs promote less vascularization compared to primary MSCs

Differentiation of iPSCs into iMSCs was confirmed by flow cytometry (Supplementary Fig. 1) based on the surface markers established by the ISCT [23]. To compare the effect of iMSCs and unreprogrammed primary MSCs on *de novo* vascularization, each cell type was mixed with endothelial cells, loaded in fibrin hydrogels, and molded within microfluidic chips. Within the chip, an inner channel holds the gel in place while two parallel channels are used as media reservoirs [24].

Confocal imaging for PECAM-1 and its 3D analysis revealed that BM-MSCs highly promote the formation of capillary-like structures by endothelial cells, while iMSCs rarely show the formation of vessels (Fig. 1A). Both vessel length and branching quantification revealed significant differences between the co-culture types (Figs. 1B and C).

3.2. Primary BM-MSCs but not iMSCs tend to associate with vessels as mural cells

A closer look at the formed vessel-like structures by TEM showed the presence of vessel lumens in the range of 5–20 μm (Fig. 2). The endothelial cells were adjacent to each other forming a ring shape, as it can be observed in native tissue. The BM-MSCs tightly surrounded the vessels with direct membrane-to-membrane contact or only with a thin layer of extracellular matrix in between. This close interaction was not found in any of the iMSCs when analyzed with minimum distances to the vessels of around 300 nm. It also revealed the presence of round structures surrounding the iMSCs (pink arrows) with the expected size (100 nm–1 μm) and a cup-shaped morphology of extracellular vesicles [22].

3.3. RNA sequencing shows a decrease of key vascularization agents in iMSCs

We compared the global gene expression profile of co-cultured endothelial cells with either primary BM-MSCs or iMSCs ($n = 3$ for each). Principal component analysis (PCA) showed the clustering of each cell type, especially of primary BM-MSCs (Fig. 3B and Supplementary Fig. 2). Comparison of both groups revealed 3739 genes with significant differences (adjusted *p*-value for multiple testing <0.05; Fig. 3C), from which 2222 genes were expressed higher in BM-MSCs and

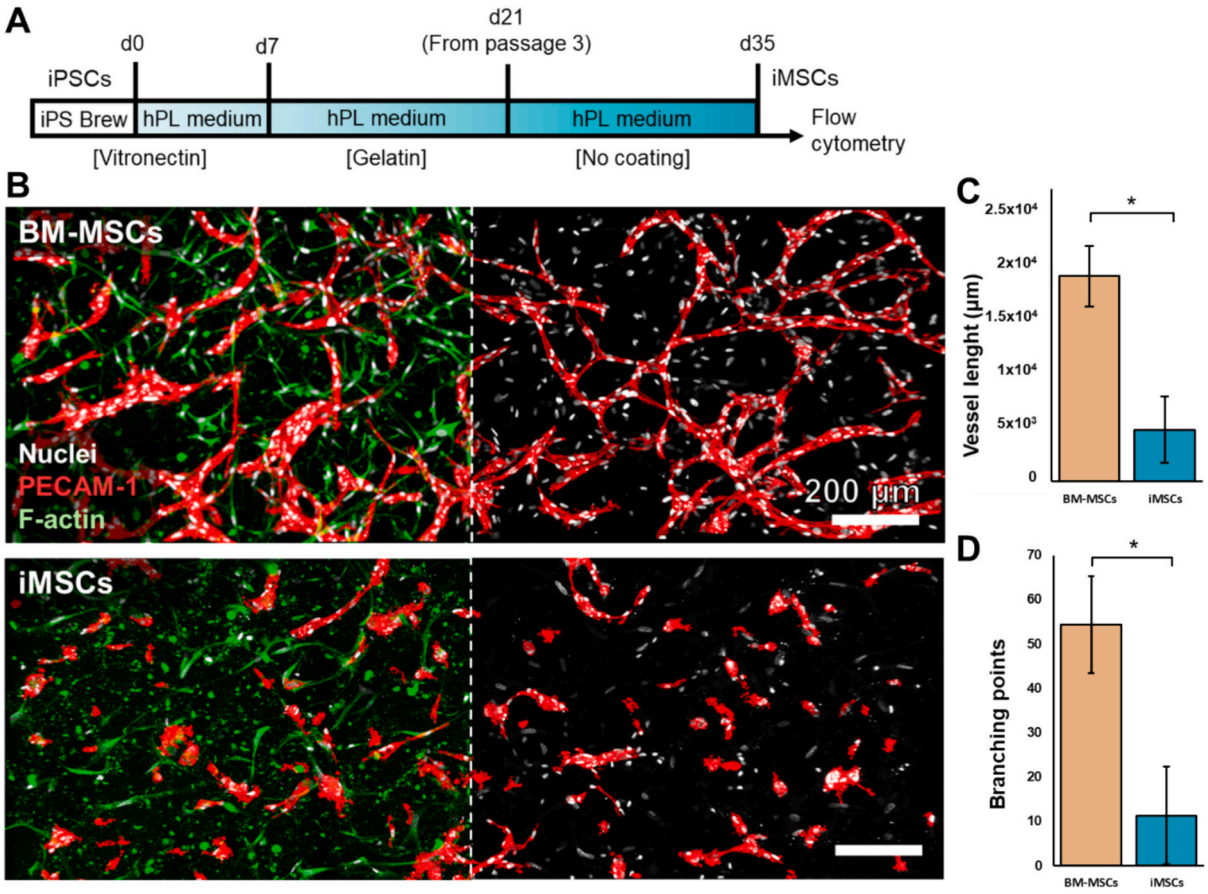

Fig. 1. Neovascularization assays with either BM-MSCs or iMSCs. (A) Confocal microscopy of the gel co-cultures showing PECAM-1$^+$ endothelial vessels in red, nuclei in white, and the F-actin of the BM-MSCs/iMSCs in green. The middle, striped line separates a composite of the three colors on the left and only red and white on the right to improve visualization, but both sides belong to the same original image. (B and C) Quantification and comparison of the vessel length ($n = 3$, unpaired *t*-test, *p*-value 0.0041) and branching points (n = 3, unpaired t-test, p-value 0.0097). (For interpretation of the references to colour in this figure legend, the reader is referred to the web version of this article.)

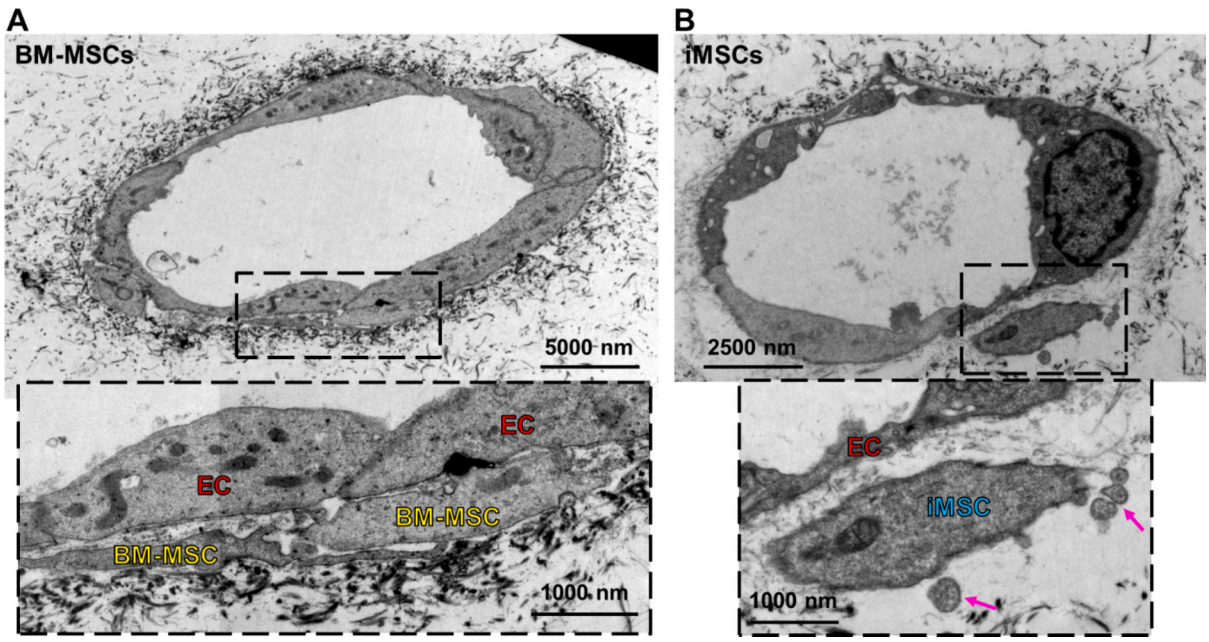

Fig. 2. Ultrastructure of the neovascularization structures. (A) BM-MSCs (yellow) closely interact with an endothelial vessel (EC, red). (B) iMSC (blue) next to a capillary. Pink arrows show extracellular vesicles surrounding the iMSC. (For interpretation of the references to colour in this figure legend, the reader is referred to the web version of this article.)

1517 were higher in iMSCs. Gene Ontology (GO) analysis of these differentially expressed genes based on the Hallmark datasets [21] showed an upregulation of metabolic and cell differentiation markers in the co-culture with iMSCs, while the one with BM-MSCs indicated increased expression of mitotic, inflammatory, and angiogenic markers (Fig. 3D). Gene Set Enrichment Analysis (GSEA) in all available datasets showed a more precise picture of the upregulated cell components and activities (Fig. 3E). Overall, iMSC co-cultures revealed an increased mitochondrial and ribosomal activity, while for BM-MSC co-cultures a heightened general signaling activity, and more specifically the one related to blood vessel formation and immune cell activation was observed.

4. Discussion

While several iPSC differentiation protocols are complex and involve small molecule mixtures, the method used in this study was based on our initial protocol for iMSC-generation which is relatively simple and cost-effective [7]. Hereby, iPSCs were re-differentiated into MSCs by switching to the initial culture medium of MSCs. This medium was only supplemented with 10 % platelet lysate of human origin, aligning with the good manufacturing practices required for cellular therapies [25].

Co-culture of these iMSCs with endothelial cells in fibrin hydrogels for ten days led to the formation of short vessel-like structures resembling native capillaries. When the resulting vascularization was compared to the one achieved by non-reprogrammed primary MSCs, it was clearly observed that iMSCs lose between 70 and 80 % of their vasculogenic potential after differentiation. Transmission electron microscopy of the gels revealed a close association of BM-MSCs to endothelial cells, resembling the mural cells wrapping around capillaries in the native bone marrow. This is in line with previous publications, and probably due to the presence of perivascular cells in BM-MSCs subpopulations [26,27]. In contrast, this close interaction was not present in iMSC co-cultures.

We resorted to RNA sequencing to unravel the molecular differences between the MSC types. Co-cultures with BM-MSCs had a higher expression than iMSCs in genes tightly related to vascularization, such as angiopoietin 2 (ANG2), nitric oxide synthase (NOS3), leptin (LEP), and fibroblast growth factor 10 (FGF10). This is clearly correlated with the significant differences in vessel formation observed by fluorescent imaging. The expression of pro-angiogenic genes in BM-MSCs has also been reported by other studies [28], positioning them and their derivatives (*i.e.* extracellular vesicles) as ideal cell therapy agents in wound healing, in which re-vascularization of the area is of the uttermost importance [29]. Overexpressed genes in iMSC co-cultures over BM-MSCs showed increases in metabolic activity, especially oxidative phosphorylation. The increased expression of epithelial-mesenchymal transition pathways in iMSCs is certainly related to the MSC re-differentiation process, in which mesenchymal genetic programs get activated [30]. The increase in mTORC1 signaling in the iMSCs may be associated with the rejuvenation and lack of senescence after reprogramming [31]. BM-MSCs, on the other hand, showed more expression of molecules related to the immune system than iMSCs, such as increased inflammation response and leukocyte activation. In contrast, the decreased immune activity of iMSCs makes them particularly relevant for diseases involving chronic inflammation or autoimmune reactions [32]. All these changes in genetic expression after the reprogramming were consistent with previous comparisons of both cell types in mono-cultures (GEO accession number GSE54766 and GSE95061) [7,12].

iMSCs fulfilled the criteria established by the ISCT [23] on surface protein expression but, although very similar, previous analysis of their gene and epigenetic profiles separates them from being identical to primary BM-MSCs [7,9]. These differences do not exclude them from being ideal cell therapy candidates, as they have solidly demonstrated their capacity to modulate immune responses and promote tissue regeneration [8,32]. However, these differences must be considered when deciding the appropriate cell therapy agent for a particular condition.

The limitations of this study include the use of bulk RNAseq instead of single-cell RNA, which may have allowed for improved differentiation between the diverse MSC subpopulation activities. Furthermore, both cell types should be also directly compared *in vivo* and in clinical trials to confirm their differential effects in neovascularization.

To the best of our knowledge, this is the first time that the role of iMSCs in neovascularization has been assessed and compared to their non-reprogrammed counterparts in a systematic way. The reduced pro-

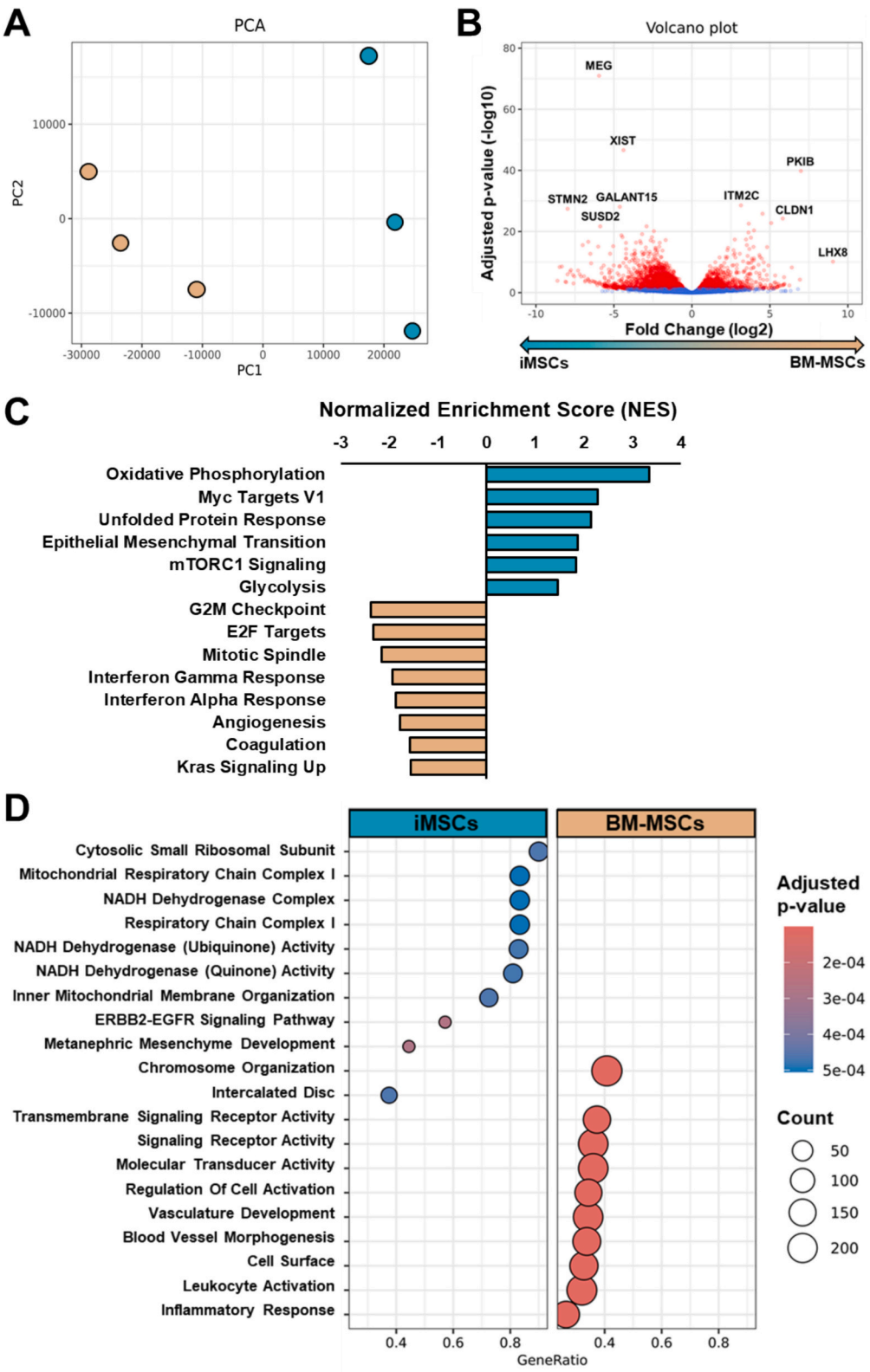

Fig. 3. RNA sequencing of the MSC co-cultures. (A) Principal component analysis (PCA) of gene expression profiles of the BM-MSCs-EC (beige) and iMSC-EC co-cultures (blue). (B) Volcano plot showing the gene expression change and adjusted *p*-values comparing both MSC co-cultures. Genes with significant differences are represented in red and non-significant ones in blue. (C) Gene ontology (GO) analysis of the significantly differently expressed genes, based on the Hallmark gene sets. Blue sets are overexpressed in iMSCs, while beige sets are overexpressed in BM-MSCs. (D) Gene set enrichment analysis (GSEA) of the significant genes for specific gene expression patterns. All data has an n of 3. (For interpretation of the references to colour in this figure legend, the reader is referred to the web version of this article.)

angiogenicity of iMSCs is highly relevant and can be an advantageous characteristic for certain therapy approaches. For instance, in osteoarthritis, increased angiogenesis promotes cartilage degradation, chondrocyte hypertrophy, and endochondral ossification [33]. New blood vessels are also often accompanied by nerve growth, which can be sensitized by inflammation, hypoxia, and mechanical stress, exacerbating the pain. Primary MSCs have been widely reported by our and other studies to activate neovascularization by, among others, the release of pro-angiogenic growth factors [10,15,34]. This can be considered a barrier to their use as cell therapeutics, although their general anti-inflammatory properties still position them as a promising treatment alternative [35]. Removing this problematic pro-angiogenicity from MSCs could significantly improve the outcome of the therapies. The same is true for several ocular diseases, such as age-related wet macular degeneration, whose pathogenesis is also tightly related to neovascularization, and in which MSC-based treatment has shown some positive results [36]. Finally, cancer has been a target of more than thirty MSC clinical trials, expecting to slow down its progression, although results have been polarizing [37]. Notably, angiogenesis is essential for cancer progression and metastasis as the inner core of the tumors rapidly becomes necrotic without irrigation [11]. Therefore, reprogrammed iMSCs may be the key to cancer cell therapy treatment.

It is worth noticing that there is no current standard in iMSC differentiation, and therefore different groups and publications can use partially or completely different protocols to reach the MSC status [32]. This leads to differences in the gene expression and activity depending on the chosen method. In case that vascularization is desired in the site of application, modification of the protocol can be explored to yield more pro-angiogenic iMSCs [8].

Overall, we demonstrated that iMSCs, a promising replacement for aged primary MSCs, may be particularly relevant in diseases where angiogenesis is undesirable, such as degenerative conditions and cancer.

CRediT authorship contribution statement

Julian Gonzalez-Rubio: Writing – original draft, Visualization, Validation, Software, Project administration, Methodology, Investigation, Formal analysis, Data curation, Conceptualization. **Kira Zeevaert:** Writing – review & editing, Visualization, Methodology. **Eva Miriam Buhl:** Writing – review & editing, Visualization, Methodology. **Michaela Schedel:** Writing – review & editing, Resources. **Stefan Jockenhoevel:** Writing – review & editing, Supervision, Resources, Funding acquisition. **Christian G. Cornelissen:** Writing – review & editing, Supervision. **Wolfgang Wagner:** Writing – review & editing, Resources, Funding acquisition. **Anja Lena Thiebes:** Writing – review & editing, Supervision, Resources, Project administration, Funding acquisition.

Funding

This study was funded by the Deutsche Forschungsgemeinschaft (DFG) (496706372; 363055819/GRK2415) and the German Federal Ministry of Education and Research (Grant numbers 031B1150B(X), and 03VP11580 (PluripotencyScreen)).

Declaration of competing interest

The authors declare the following financial interests/personal relationships which may be considered as potential competing interests: W.W. is involved in the company Cygenia (www.cygenia.com) which can provide services for epigenetic analysis to other scientists, including Epi-Pluri-Score analysis. The other authors declare that they have no known competing financial interests or personal relationships that could have appeared to influence the work reported in this paper.

Acknowledgements

We wish to thank the Orthopedic Clinic for providing the femoral heads (Univ.-Prof. Dr. Hildebrand). We also want to thank the Department of Gynecology and Perinatal Medicine (Univ.-Prof. Dr. Stickeler) and the Centralized Biomaterial Bank of the RWTH Aachen University (cBMB) for providing the human umbilical cords. This work was supported by the Flow Cytometry Facility, the Confocal Microscopy Facility, and the Genomics Facility of the Interdisciplinary Center for Clinical Research (IZKF) Aachen, within the Faculty of Medicine at RWTH Aachen University.

Appendix A. Supplementary data

Supplementary data to this article can be found online at https://doi.org/10.1016/j.lfs.2024.123298.

Data availability

Data will be made available on request.

References

[1] W. Wagner, F. Wein, A. Seckinger, M. Frankhauser, U. Wirkner, U. Krause, J. Blake, C. Schwager, V. Eckstein, W. Ansorge, A.D. Ho, Comparative characteristics of mesenchymal stem cells from human bone marrow, adipose tissue, and umbilical cord blood, Exp. Hematol. 33 (2005) 1402–1416, https://doi.org/10.1016/j.exphem.2005.07.003.

[2] A.I. Caplan, Mesenchymal stem cells, J. Orthop. Res. 9 (1991) 641–650, https://doi.org/10.1002/jor.1100090504.

[3] D.G. Phinney, Alexander Friedenstein, Mesenchymal stem cells, shifting paradigms and euphemisms, Bioengineering (Basel) 11 (2024), https://doi.org/10.3390/bioengineering11060534.

[4] D. Jovic, Y. Yu, D. Wang, K. Wang, H. Li, F. Xu, C. Liu, J. Liu, Y. Luo, A brief overview of global trends in MSC-based cell therapy, Stem Cell Rev. Rep. 18 (2022) 1525–1545, https://doi.org/10.1007/s12015-022-10369-1.

[5] U. Galderisi, G. Peluso, G. Di Bernardo, Clinical trials based on mesenchymal stromal cells are exponentially increasing: where are we in recent years? Stem Cell Rev. Rep. 18 (2022) 23–36, https://doi.org/10.1007/s12015-021-10231-w.

[6] K. Kelly, A.J.C. Bloor, J.E. Griffin, R. Radia, D.T. Yeung, J.E.J. Rasko, Two-year safety outcomes of iPS cell-derived mesenchymal stromal cells in acute steroid-resistant graft-versus-host disease, Nat. Med. 30 (2024) 1556–1558, https://doi.org/10.1038/s41591-024-02990-z.

[7] J. Frobel, H. Hemeda, M. Lenz, G. Abagnale, S. Joussen, B. Denecke, T. Sarić, M. Zenke, W. Wagner, Epigenetic rejuvenation of mesenchymal stromal cells derived from induced pluripotent stem cells, Stem Cell Reports 3 (2014) 414–422, https://doi.org/10.1016/j.stemcr.2014.07.003.

[8] L.-S. Spitzhorn, M. Megges, W. Wruck, M.S. Rahman, J. Otte, Ö. Degistirici, R. Meisel, R.V. Sorg, R.O.C. Oreffo, J. Adjaye, Human iPSC-derived MSCs (iMSCs) from aged individuals acquire a rejuvenation signature, Stem Cell Res Ther 10 (2019) 100, https://doi.org/10.1186/s13287-019-1209-x.

[9] E. Fernandez-Rebollo, J. Franzen, R. Goetzke, J. Hollmann, A. Ostrowska, M. Oliverio, T. Sieben, B. Rath, J.-W. Kornfeld, W. Wagner, Senescence-associated metabolomic phenotype in primary and iPSC-derived mesenchymal stromal cells, Stem Cell Rep. 14 (2020) 201–209, https://doi.org/10.1016/j.stemcr.2019.12.012.

[10] A.E. Luengen, M. Cheremkhina, J. Gonzalez-Rubio, J. Weckauf, C. Kniebs, H. Uebner, E.M. Buhl, C. Taube, C.G. Cornelissen, T. Schmitz-Rode, S. Jockenhoevel, A.L. Thiebes, Bone marrow derived mesenchymal stromal cells promote vascularization and ciliation in airway mucosa tri-culture models in vitro, Front. Bioeng. Biotechnol. 10 (2022) 872275, https://doi.org/10.3389/fbioe.2022.872275.

[11] G. Eelen, L. Treps, X. Li, P. Carmeliet, Basic and therapeutic aspects of angiogenesis updated, Circ. Res. 127 (2020) 310–329, https://doi.org/10.1161/CIRCRESAHA.120.316851.

[12] R. Goetzke, J. Franzen, A. Ostrowska, M. Vogt, A. Blaeser, G. Klein, B. Rath, H. Fischer, M. Zenke, W. Wagner, Does soft really matter? Differentiation of induced pluripotent stem cells into mesenchymal stromal cells is not influenced by soft hydrogels, Biomaterials 156 (2018) 147–158, https://doi.org/10.1016/j.biomaterials.2017.11.035.

[13] M. Lenz, R. Goetzke, A. Schenk, C. Schubert, J. Veeck, H. Hemeda, S. Koschmieder, M. Zenke, A. Schuppert, W. Wagner, Epigenetic biomarker to support classification into pluripotent and non-pluripotent cells, Sci. Rep. 5 (2015) 8973, https://doi.org/10.1038/srep08973.

[14] M. Lohmann, G. Walenda, H. Hemeda, S. Joussen, W. Drescher, S. Jockenhoevel, G. Hutschenreuter, M. Zenke, W. Wagner, Donor age of human platelet lysate affects proliferation and differentiation of mesenchymal stem cells, PLoS One 7 (2012) e37839, https://doi.org/10.1371/journal.pone.0037839.

[15] A. Mykuliak, A. Yrjänäinen, A.-J. Mäki, A. Gebraad, E. Lampela, M. Kääriäinen, T.-K. Pakarinen, P. Kallio, S. Miettinen, H. Vuorenpää, Vasculogenic potency of bone marrow- and adipose tissue-derived mesenchymal stem/stromal cells results in differing vascular network phenotypes in a microfluidic chip, Front. Bioeng. Biotechnol. 10 (2022) 764237, https://doi.org/10.3389/fbioe.2022.764237.
[16] P. Di Tommaso, M. Chatzou, E.W. Floden, P.P. Barja, E. Palumbo, C. Notredame, Nextflow enables reproducible computational workflows, Nat. Biotechnol. 35 (2017) 316–319, https://doi.org/10.1038/nbt.3820.
[17] P.A. Ewels, A. Peltzer, S. Fillinger, H. Patel, J. Alneberg, A. Wilm, M.U. Garcia, P. Di Tommaso, S. Nahnsen, The nf-core framework for community-curated bioinformatics pipelines, Nat. Biotechnol. 38 (2020) 276–278, https://doi.org/10.1038/s41587-020-0439-x.
[18] F. Krueger, F. James, P. Ewels, E. Afyounian, M. Weinstein, B. Schuster-Boeckler, G. Hulselmans, sclamons, Felix Krueger/TrimGalore: v0.6.10 - Add Default Decompression Path, 2023, https://doi.org/10.5281/zenodo.7598955.
[19] A. Dobin, C.A. Davis, F. Schlesinger, J. Drenkow, C. Zaleski, S. Jha, P. Batut, M. Chaisson, T.R. Gingeras, STAR: ultrafast universal RNA-seq aligner, Bioinformatics 29 (2013) 15–21, https://doi.org/10.1093/bioinformatics/bts635.
[20] M.I. Love, W. Huber, S. Anders, Moderated estimation of fold change and dispersion for RNA-seq data with DESeq2, Genome Biol. 15 (2014) 550, https://doi.org/10.1186/s13059-014-0550-8.
[21] A. Liberzon, C. Birger, H. Thorvaldsdóttir, M. Ghandi, J.P. Mesirov, P. Tamayo, The molecular signatures database (MSigDB) hallmark gene set collection, Cell Syst. 1 (2015) 417–425, https://doi.org/10.1016/j.cels.2015.12.004.
[22] G. Yu, L.-G. Wang, Y. Han, Q.-Y. He, clusterProfiler: an R package for comparing biological themes among gene clusters, OMICS 16 (2012) 284–287, https://doi.org/10.1089/omi.2011.0118.
[23] M. Dominici, K. Le Blanc, I. Mueller, I. Slaper-Cortenbach, F. Marini, D. Krause, R. Deans, A. Keating, D. Prockop, E. Horwitz, Minimal criteria for defining multipotent mesenchymal stromal cells. The International Society for Cellular Therapy position statement, Cytotherapy 8 (2006) 315–317, https://doi.org/10.1080/14653240600855905.
[24] K. Haase, R.D. Kamm, Advances in on-chip vascularization, Regen. Med. 12 (2017) 285–302, https://doi.org/10.2217/rme-2016-0152.
[25] M. Oeller, S. Laner-Plamberger, L. Krisch, E. Rohde, D. Strunk, K. Schallmoser, Human platelet lysate for good manufacturing practice-compliant cell production, Int. J. Mol. Sci. 22 (2021), https://doi.org/10.3390/ijms22105178.
[26] A. Blocki, Y. Wang, M. Koch, P. Peh, S. Beyer, P. Law, J. Hui, M. Raghunath, Not all MSCs can act as pericytes: functional in vitro assays to distinguish pericytes from other mesenchymal stem cells in angiogenesis, Stem Cells Dev. 22 (2013) 2347–2355, https://doi.org/10.1089/scd.2012.0415.
[27] S. Ruoss, C.A. Nasamran, S.T. Ball, J.L. Chen, K.N. Halter, K.A. Bruno, T. C. Whisenant, J.N. Parekh, S.N. Dorn, M.C. Esparza, S.N. Bremner, K.M. Fisch, A. J. Engler, S.R. Ward, Comparative single-cell transcriptional and proteomic atlas of clinical-grade injectable mesenchymal source tissues, Sci. Adv. 10 (2024) eadn2831, https://doi.org/10.1126/sciadv.adn2831.
[28] S.M. Watt, F. Gullo, M. van der Garde, D. Markeson, R. Camicia, C.P. Khoo, J. J. Zwaginga, The angiogenic properties of mesenchymal stem/stromal cells and their therapeutic potential, Br. Med. Bull. 108 (2013) 25–53, https://doi.org/10.1093/bmb/ldt031.
[29] H. Sorg, D.J. Tilkorn, U. Mirastschijski, J. Hauser, R. Kraemer, Panta rhei: neovascularization, angiogenesis and nutritive perfusion in wound healing, Eur. Surg. Res. 59 (2018) 232–241, https://doi.org/10.1159/000492410.
[30] T. Winston, Y. Song, H. Shi, J. Yang, M. Alsudais, M.I. Kontaridis, Y. Wu, T. R. Gaborski, Q. Meng, R.N. Cooney, Z. Ma, Lineage-specific mesenchymal stromal cells derived from human iPSCs showed distinct patterns in transcriptomic profile and extracellular vesicle production, Adv. Sci. (Weinh) 11 (2024) e2308975, https://doi.org/10.1002/advs.202308975.
[31] V. Panwar, A. Singh, M. Bhatt, R.K. Tonk, S. Azizov, A.S. Raza, S. Sengupta, D. Kumar, M. Garg, Multifaceted role of mTOR (mammalian target of rapamycin) signaling pathway in human health and disease, Sig Transduct Target Ther 8 (2023) 375, https://doi.org/10.1038/s41392-023-01608-z.
[32] X. Zhou, J. Liu, F. Wu, J. Mao, Y. Wang, J. Zhu, K. Hong, H. Xie, B. Li, X. Qiu, X. Xiao, C. Wen, The application potential of iMSCs and iMSC-EVs in diseases, Front. Bioeng. Biotechnol. 12 (2024) 1434465, https://doi.org/10.3389/fbioe.2024.1434465.
[33] Y.A. Pei, S. Chen, M. Pei, The essential anti-angiogenic strategies in cartilage engineering and osteoarthritic cartilage repair, Cell. Mol. Life Sci. 79 (2022) 71, https://doi.org/10.1007/s00018-021-04105-0.
[34] D. Todorova, S. Simoncini, R. Lacroix, F. Sabatier, F. Dignat-George, Extracellular vesicles in angiogenesis, Circ. Res. 120 (2017) 1658–1673, https://doi.org/10.1161/CIRCRESAHA.117.309681.
[35] G. Copp, K.P. Robb, S. Viswanathan, Culture-expanded mesenchymal stromal cell therapy: does it work in knee osteoarthritis? A pathway to clinical success, Cell. Mol. Immunol. 20 (2023) 626–650, https://doi.org/10.1038/s41423-023-01020-1.
[36] V. Holan, K. Palacka, B. Hermankova, Mesenchymal stem cell-based therapy for retinal degenerative diseases: experimental models and clinical trials, Cells 10 (2021), https://doi.org/10.3390/cells10030588.
[37] T. Lan, M. Luo, X. Wei, Mesenchymal stem/stromal cells in cancer therapy, J. Hematol. Oncol. 14 (2021) 195, https://doi.org/10.1186/s13045-021-01208-w.